Decentralised Finance and Automated Market Making: Predictable Loss and Optimal Liquidity Provision

Álvaro Cartea[a,b], Fayçal Drissi[a], Marcello Monga[a,b]

[a] *Oxford-Man Institute of Quantitative Finance, Oxford, UK*
[b] *Mathematical Institute, University of Oxford, Oxford, UK*

Abstract

Constant product markets with concentrated liquidity (CL) are the most popular type of automated market makers. In this paper, we characterise the continuous-time wealth dynamics of strategic LPs who dynamically adjust their range of liquidity provision in CL pools. Their wealth results from fee income and the value of their holdings in the pool. Next, we derive a self-financing and closed-form optimal liquidity provision strategy where the width of the LP's liquidity range is determined by the profitability of the pool (provision fees minus gas fees), the predictable losses (PL) of the LP's position, and concentration risk. Concentration risk refers to the decrease in fee revenue if the marginal exchange rate (akin to the midprice in a limit order book) in the pool exits the LP's range of liquidity. When the marginal rate is driven by a stochastic drift, we show how to optimally skew the range of liquidity to increase fee revenue and profit from the expected changes in the marginal rate. Finally, we use Uniswap v3 data to show that, on average, LPs have traded at a significant loss, and to show that the out-of-sample performance of our strategy is superior to the historical performance of LPs in the pool we consider.

Keywords: Decentralised finance, automated market making, concentrated liquidity, algorithmic trading, market making, stochastic control, predictable loss, impermanent loss, signals.

We are grateful to Tarek Abou Zeid, Álvaro Arroyo, Sam Cohen, Patrick Chang, Mihai Cucuringu, Olivier Guéant, Anthony Ledford, Andre Rzym, and Leandro Sánchez-Betancourt, for insightful comments. The authors thank the Fintech Dauphine Chair, in partnership with Mazars and Crédit Agricole CIB, for their financial support. We are also grateful to seminar participants at Oxford, the OMI, the Oxford Victoria Seminar, and the DeFi Research Group. FD is grateful to the Oxford-Man Institute's generosity and hospitality. MM acknowledges financial support from the EPSRC Centre for Doctoral Training in Mathematics of Random Systems: Analysis, Modelling and Simulation (EP/S023925/1).

Electronic copy available at: https://ssrn.com/abstract=4273989

1. Introduction

Traditional electronic exchanges are organised around LOBs to clear demand and supply of liquidity. In contrast, the takers and providers of liquidity in constant function markets (CFMs) interact in liquidity pools; liquidity providers (LPs) deposit their assets in the liquidity pool and liquidity takers (LTs) exchange assets directly with the pool. At present, constant product markets (CPMs) with concentrated liquidity (CL) are the most popular type of CFM, with Uniswap v3 as a prime example; see Adams et al. (2021). In CPMs with CL, LPs specify the rate intervals (i.e., tick ranges) over which they deposit their assets, and this liquidity is counterparty to trades of LTs when the marginal exchange rate of the pool is within the liquidity range of the LPs. When LPs deposit liquidity, fees paid by LTs accrue and are paid to LPs when they withdraw their assets from the pool. The amount of fees accrued to LPs is proportional to the share of liquidity they hold in the pool.

Existing research characterises the losses of LPs, but does not offer tools for strategic liquidity provision. In this paper, we study strategic liquidity provision in CPMs with CL. We derive the continuous-time dynamics of the wealth of LPs which consists of the position they hold in the pool (position value) and fee income. The width of the range where the assets are deposited affects the value of the LP's position in the pool; specifically, we show that the predictable loss (PL) incurred by LPs increases as the width of the liquidity range decreases. PL measures the unhedgeable losses of LPs stemming from the depreciation of their holdings in the pool and from the opportunity costs from locking their assets in the pool; see Cartea et al. (2023). Also, we show that fee income is subject to a tradeoff between the width of the LP's liquidity range and the volatility of the marginal rate in the pool. More precisely, CL increases fee revenue when the rate is in the range of the LP, but also increases *concentration risk*. Concentration risk refers to the risk that the LP faces when her position is concentrated in narrow ranges; the LP stops collecting fees when the rate exits the range of her position.

We derive an optimal dynamic strategy to provide liquidity in a CPM with CL. In our model, the LP maximises the expected utility of her terminal wealth, which consists of the accumulated trading fees and the gains and losses from the market making strategy. The dynamic strategy controls the width and the skew of liquidity that targets the marginal exchange rate. For the particular case of log-utility, we obtain the strategy in closed-form and show how the solution balances the opposing effects between PL and fee collection. When volatility increases, PL increases, so there is an incentive for the LP to widen the range of liquidity provision to reduce the strategy's exposure to PL. In particular, in the extreme case of very high volatility, the LP must withdraw from the pool because the exposure to PL is too high. Also, when there is an increase in the potential

Electronic copy available at: https://ssrn.com/abstract=4273989

provision fees that the LP may collect because of higher liquidity taking activity, the strategy balances two opposing forces. One, there is an incentive to increase fee collection by concentrating the liquidity of the LP in a tight range around the exchange rate of the pool. Two, there is a limit to how concentrated is the liquidity posted by the LP in the pool because the LP does not collect fees if the exchange rate exits the LP's liquidity range. Finally, when the dynamics of the marginal exchange rate are driven by a stochastic drift (e.g., a predictive signal), the strategy skews the range of liquidity to increase fee revenue by capturing the LT trading flow and to increase the position value by profiting from the excepted changes in the marginal rate.

Finally, we use Uniswap v3 data to motivate our model and to test the performance of the strategy we derive. The LP and LT data are from the pool ETH/USDC (Ethereum and USD coin) between the inception of the pool on 5 May 2021 and 18 August 2022. To illustrate the performance of the strategy we use in-sample data to estimate model parameters and out-of-sample data to test the strategy. Our analysis of the historical transactions in Uniswap v3 shows that LPs have traded at a significant loss, on average, in the ETH/USDC pool. We show that the out-of-sample performance of our strategy is considerably superior to the average LP performance we observe in the ETH/USDC pool.

Early works on AMMs are in Chiu and Koeppl (2019), Angeris et al. (2021), Lipton and Treccani (2021). Some works in the literature study strategic liquidity provision in CFMs and CPMs with CL. Fan et al. (2023) propose a liquidity provision strategy in pools with CL, Heimbach et al. (2022) discuss the tradeoff between risks and returns that LPs face in Uniswap v3, Cartea et al. (2023) study the predictable losses of LPs in a continuous-time setup, Milionis et al. (2023) study the impact of fees on the profits of arbitrageurs in CFMs, and Fukasawa et al. (2023) study the hedging of the impermanent losses of LPs.

Our work is related to the algorithmic trading and optimal market making literature. Early works on liquidity provision in traditional markets are Ho and Stoll (1983) and Avellaneda and Stoikov (2008), with extensions in many directions; see Cartea et al. (2014, 2017), Guéant (2017), Bergault et al. (2021), Drissi (2022). We refer the reader to Cartea et al. (2015) and Guéant (2016) for a comprehensive review of algorithmic trading models for takers and makers of liquidity in traditional markets. Also, our work is related to those by Cartea et al. (2018), Barger and Lorig (2019), Cartea and Wang (2020), Donnelly and Lorig (2020), Forde et al. (2022), Bergault et al. (2022) who implement market signals in algorithmic trading strategies.

The remainder of the paper proceeds as follows. Section 2 describes CL pools. Section 3 studies the continuous-time dynamics of the wealth of LPs as a result of the position value in Subsection 3.1 and the fee revenue in Subsection 3.2. In particular, we use Uniswap v3 data to

Electronic copy available at: https://ssrn.com/abstract=4273989

study the fee revenue component of the LP's wealth and our results motivate the assumptions we make in our model. Section 4 introduces our liquidity provision model and uses stochastic control to derive a closed-form optimal strategy. Next, we study how the strategy controls the width and the skew of the liquidity range as a function of the pool's profitability, PL, concentration risk, and the drift in the marginal rate. Finally, Section 5 uses Uniswap v3 data to test the performance of the strategy and showcases its superior performance.

2. Concentrated liquidity

Consider a reference asset X and a risky asset Y which is valued in units of X. Assume there is a pool that makes liquidity for the pair of assets X and Y, and denote by Z the marginal exchange rate of asset Y in units of asset X in the pool. In a traditional CPM such as Uniswap v2, the trading function, which links the state of the pool before and after a trade is executed, is $f\left(q^X, q^Y\right) = q^X \times q^Y = \kappa^2$ where q^X and q^Y are the quantities of asset X and Y that constitute the *reserves* in the pool, and κ is the depth of the pool. The marginal exchange rate is $Z = q^X/q^Y$, and the execution rate for a quantity y is $\tilde{Z}\left(y\right) = Z - Z^{3/2}\, y/\kappa$. In traditional CPMs, liquidity provision operations do not impact the marginal rate of the pool, so when an LP deposits the quantities x and y of assets X and Y, the condition $q^X/q^Y = (q^X + x)/(q^Y + y)$ must be satisfied; see Cartea et al. (2022).

Figure 1 illustrates the geometry of a CPM. The level function $\varphi(q^Y) = \kappa^2/q^Y$ indicates the various combinations of quantity q^X and quantity q^Y that lead to the same pool depth. Assume the reserves in the pool are the coordinates of point B in Figure 1. The marginal rate Z is the absolute value of the slope of the tangent $q^X/q^Y = \kappa^2/\left(q^Y\right)^2$ at point B; equivalently, Z is the slope of the ray $0B$. When LTs trade, the reserves in the pool move along the level curve (e.g., from B to C or from B to A), and when LPs provide liquidity, the level curve moves up along the ray $(0B)$.

In CPMs with CL, LPs specify a range of rates $(Z^\ell, Z^u]$ in which their assets can be counterparty to liquidity taking trades. Here, Z^ℓ and Z^u take values in a finite set $\{Z^1, \ldots, Z^N\}$, the elements of the set are called ticks, and the range $(Z^i, Z^{i+1}]$ between two consecutive ticks is a *tick range* which represents the smallest possible liquidity range; see Drissi (2023) for a description of the mechanics of CL.[1]

The assets that the LP deposits in a range $(Z^\ell, Z^u]$ provide the liquidity that supports marginal rate movements between Z^ℓ and Z^u. The quantities x and y that the LP provides verify the key

[1] In LOBs, a tick is the smallest price increment.

Electronic copy available at: https://ssrn.com/abstract=4273989

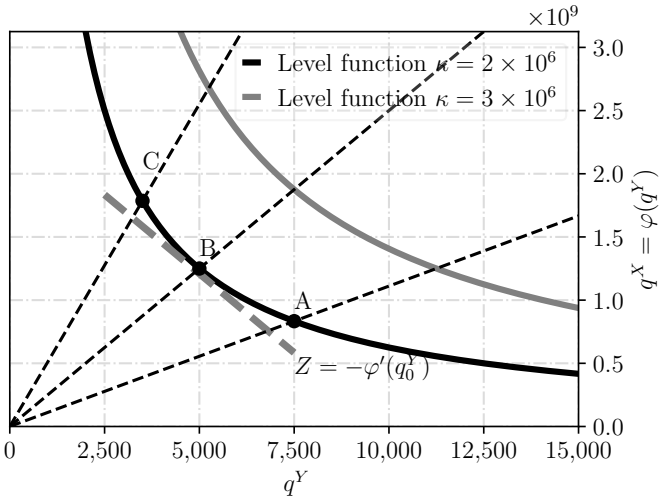

Figure 1: Geometry of CPMs: level function $x = \varphi(y) = \kappa^2/y$ for two values of the pool depth κ.

formulae

$$\begin{cases} x = 0 & \text{and} \quad y = \tilde{\kappa}\left(\left(Z^{\ell}\right)^{-1/2} - \left(Z^{u}\right)^{-1/2}\right) & \text{if } Z \leq Z^{\ell}, \\ x = \tilde{\kappa}\left(Z^{1/2} - \left(Z^{\ell}\right)^{1/2}\right) & \text{and} \quad y = \tilde{\kappa}\left(Z^{-1/2} - \left(Z^{u}\right)^{-1/2}\right) & \text{if } Z^{\ell} < Z \leq Z^{u}, \\ x = \tilde{\kappa}\left(\left(Z^{u}\right)^{1/2} - \left(Z^{\ell}\right)^{1/2}\right) & \text{and} \quad y = 0 & \text{if } Z > Z^{u}, \end{cases} \tag{1}$$

where $\tilde{\kappa}$ is the depth of the LP's liquidity in the pool. The depth $\tilde{\kappa}$ remains constant unless the LP provides additional liquidity or withdraws her liquidity. When the rate Z changes, the equations in (1) and the prevailing marginal rate Z determine the holdings of the LP in the pool, in particular, they determine the quantities of each asset received by the LP when she withdraws her liquidity.

Within each tick range, the constant product formula determines the dynamics of the marginal rate, where the depth κ is the total depth of liquidity in that tick range. To obtain the total depth in a tick range, one sums the depths of the individual liquidity positions in the same tick range. When a liquidity taking trade is large, so the marginal rate crosses the boundary of a tick range, the pool executes two separate trades with potentially different depths for the constant product formula. Figure 2 depicts the geometry of CPMMs with CL for two adjacent tick ranges, each with a different value of the depth κ. In CPMMs without CL, the level function is a hyperbola, and in CPMMs with CL, it is a series of adjacent segments of hyperbolas, each corresponding to a given value of the depth.

If an LP's liquidity position with depth $\tilde{\kappa}$ is in a tick range where the total depth of liquidity is

Electronic copy available at: https://ssrn.com/abstract=4273989

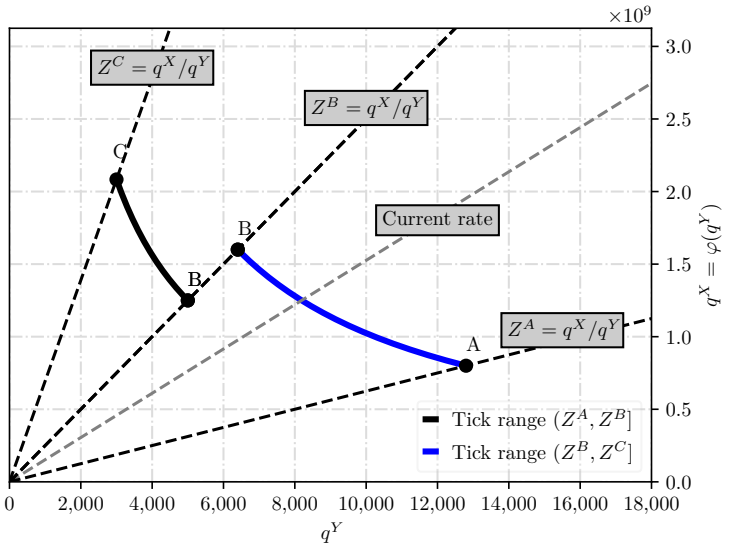

Figure 2: Geometry of CPMMs with CL: two adjacent tick ranges $(Z^B, Z^C]$ and $(Z^A, Z^B]$ with different liquidity depth.

κ, then for every liquidity taking trade that pays an amount p of fees, the LP earns the amount

$$\tilde{p} = \frac{\tilde{\kappa}}{\kappa}\, p\, \mathbb{1}_{Z^\ell < Z \leq Z^u}\,. \tag{2}$$

Thus, the larger the position depth $\tilde{\kappa}$, the higher is the proportion of fees that the LP earns; e.g., if the LP is the only provider of liquidity in the range $(Z^\ell, Z^u]$ then $\kappa = \tilde{\kappa}$, so the LP collects all the fees in that range. The equations in (1) imply that for equal wealth, narrow liquidity ranges increase the value of $\tilde{\kappa}$. However, LPs that maximise fee revenue in a tick range face concentration risk.

To illustrate concentration risk, consider the following example. Two LPs have the same initial wealth $\tilde{x}$. One LP provides liquidity over the one-tick range $(Z^i, Z^{i+1}]$ with depth κ_1, and the other LP provides liquidity with depth κ_2 over a range $(Z^i, Z^{i+2}]$ that consists of two tick ranges. The equations in (1) show that the depth of the position of the LP who concentrates her liquidity over one tick range is approximately twice the depth of the liquidity held by the second LP; see Cartea et al. (2022, 2023) for more details. However, when the rate Z is in the tick range $(Z^{i+1}, Z^{i+2}]$, the first LP's liquidity is inactive and does not earn fees, and only the second LP's liquidity facilitates trades. Figure 3 shows the position depth of an LP who uses the same wealth to provide liquidity over ranges of 1, 3, and 5 ticks.

Electronic copy available at: https://ssrn.com/abstract=4273989

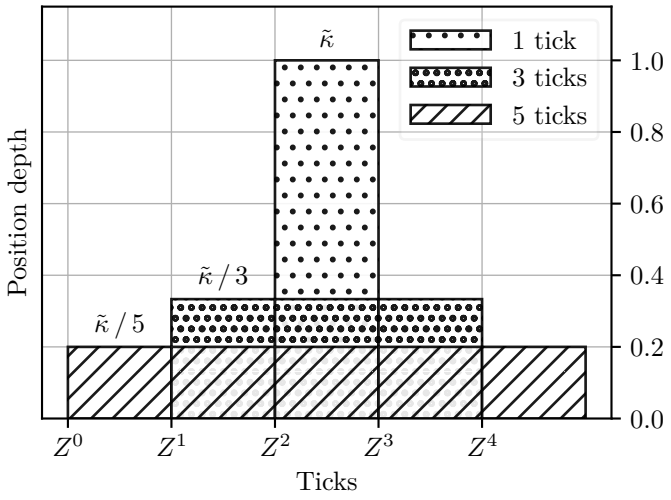

Figure 3: Position depth for three LP ranges. The first is concentrated over a range of one tick, the second over a range of three ticks, and the last over a range of five ticks.

3. The wealth of liquidity providers in CL pools

In this section, we consider a strategic LP who dynamically tracks the marginal rate Z. In our model, the LP's position is self-financed, so she does not deposit nor withdraw additional assets throughout a investment window $[0, T]$. Throughout the investment window, the LP repeatedly withdraws her liquidity and collects the accumulated fees, then uses her wealth, i.e., the collected fees and the assets she withdraws, to deposit liquidity in a new range. In the remainder of this work, we work in a filtered probability space $\big(\Omega, \mathcal{F}, \mathbb{P}; \mathbb{F} = (\mathcal{F}_t)_{t\in[0,T]}\big)$ that satisfies the usual conditions, where $\mathbb{F}$ is the natural filtration generated by the collection of observable stochastic processes that we define below.

We assume that the marginal exchange rate in the pool $(Z_t)_{t\in[0,T]}$ is driven by a stochastic drift $(\mu_t)_{t\in[0,T]}$ and we write

$$\mathrm{d}Z_t = \mu_t\, Z_t\, \mathrm{d}t + \sigma\, Z_t\, \mathrm{d}W_t\,, \tag{3}$$

where the volatility parameter σ is a nonnegative constant and $(W_t)_{t\in[0,T]}$ is a standard Brownian motion independent of μ. We assume that μ is càdlàg with finite second moment, i.e., $\mathbb{E}\,[\mu_s^2] < \infty$ for $t \le s \le T$.

Consider an LP with initial wealth $\tilde{x}_0$, in units of X, and an investment horizon $[0, T]$, with $T > 0$. At time $t = 0$, she deposits quantities (x_0, y_0) in the range $\big(Z^\ell, Z^u\big]$ so the initial depth of her position is $\tilde{\kappa}_0$, and the value of her initial position, marked-to-market in units of X, is

Electronic copy available at: https://ssrn.com/abstract=4273989

$\tilde{x}_0 = x_0 + y_0\, Z_0$. The dynamics of the LP's wealth consist of the position value and fee revenue. We introduce the wealth process $(\tilde{x}_t = \alpha_t + p_t)_{t\in[0,T]}$, which we mark-to-market in units of the reference asset X, with $\tilde{x}_0 > 0$ known and recall that $(\alpha_t)_{t\in[0,T]}$ is the value of the LP's holdings in the pool and $(p_t)_{t\in[0,T]}$ is the fee revenue. At any time t, the LP uses her wealth $\tilde{x}_t$ to provide liquidity. Next, Subsection 3.1 studies the dynamics of the LP's position in the pool and Subsection 3.2 studies the dynamics of the LP's fee revenue.

3.1. Position value

In this section, we focus our analysis on the *position value* α. Throughout the investment window $[0,T]$, the holdings $(x_t, y_t)_{t\in[0,T]}$ of the LP change because the marginal rate Z changes and because she continuously adjusts her liquidity range around Z. More precisely, to make markets optimally, the LP controls the values of $\left(\delta^\ell_t\right)_{t\in[0,T]}$ and $(\delta^u_t)_{t\in[0,T]}$ which determine the dynamic liquidity provision boundaries $\left(Z^\ell_t\right)_{t\in[0,T]}$ and $(Z^u_t)_{t\in[0,T]}$ as follows:

$$\begin{cases} \left(Z^u_t\right)^{1/2} = & Z_t^{1/2} / \left(1 - \delta^u_t/2\right), \\ \left(Z^\ell_t\right)^{1/2} = & Z_t^{1/2} \left(1 - \delta^\ell_t/2\right), \end{cases} \tag{4}$$

where $\delta^\ell \in (-\infty, 2]$, $\delta^u \in [-\infty, 2)$, and $\delta^\ell\, \delta^u/2 < \delta^\ell + \delta^u$ because $0 \leq Z^\ell < Z^u < \infty$. Below, our liquidity provision model requires that $Z_t \in (Z^\ell_t, Z^u_t]$ so $\delta^\ell \in (0,2]$, $\delta^u \in [0,2)$, and $\delta^\ell\, \delta^u/2 < \delta^\ell + \delta^u$.

Recall that in practice, Z^ℓ and Z^u take values in a finite set of ticks, so δ^ℓ and δ^u also take values in a finite set. In the liquidity provision problem of Section 4, we use stochastic control techniques to derive an optimal strategy where the controls δ^ℓ and δ^u are continuous, so we round the values of Z^ℓ and Z^u to the nearest ticks in the performance analysis of Section 5.

In the remainder of this paper we define the *spread* δ_t of the LP's position as

$$\delta_t = \delta^u_t + \delta^\ell_t, \tag{5}$$

and for small position spreads, we use the approximation

$$\left(Z^u_t - Z^\ell_t\right) \Big/ Z_t = \left(1 - \delta^u_t/2\right)^{-2} - \left(1 - \delta^\ell_t/2\right)^2 \approx \delta_t.$$

We assume that the marginal rate process $(Z_t)_{t\in[0,T]}$ follows the dynamics (3). Cartea et al. (2023) show that the holdings in assets X and Y in the pool for an LP who follows an arbitrary

Electronic copy available at: https://ssrn.com/abstract=4273989

strategy $\left(Z_t^\ell, Z_t^u\right)$ are given by

$$x_t = \frac{\delta_t^\ell}{\delta_t^\ell + \delta_t^u}\,\alpha_t \quad \text{and} \quad y_t = \frac{\delta_t^u}{Z_t\left(\delta_t^\ell + \delta_t^u\right)}\,\alpha_t\,, \tag{6}$$

so the value $(\alpha_t)_{t\in[0,T]}$ of her position follows the dynamics

$$\begin{aligned} \mathrm{d}\alpha_t &= \tilde{x}_t\left(\frac{1}{\delta_t^\ell + \delta_t^u}\right)\left(-\frac{\sigma^2}{2}\,\mathrm{d}t + \mu_t\,\delta_t^u\,\mathrm{d}t + \sigma\,\delta_t^u\,\mathrm{d}W_t\right) \\ &= \mathrm{dPL}_t + \tilde{x}_t\left(\frac{1}{\delta_t^\ell + \delta_t^u}\right)\left(\mu_t\,\delta_t^u\,\mathrm{d}t + \sigma\,\delta_t^u\,\mathrm{d}W_t\right)\,, \end{aligned} \tag{7}$$

where the predictable and negative component $\mathrm{PL}_t = -\frac{\sigma^2}{2}\int_0^t \frac{\tilde{x}_s}{\delta_s}\,\mathrm{d}s$ is the PL of the LP's position which scales with the volatility of the marginal rate. The dynamics in (7) also show that a larger position spread δ reduces PL and the overall risk of the LP's position in the pool; see Cartea et al. (2023).

For a fixed value of the spread $\delta_t = \delta_t^\ell + \delta_t^u$, the dynamics in (7) show that if $\mu_t \geq 0$, then the LP increases her expected wealth by increasing the value δ^u, i.e., by skewing her range of liquidity to the right. However, note that the quadratic variation of the LP's position value is $\mathrm{d}\langle\alpha,\alpha\rangle_t = \tilde{x}_t^2\,\sigma^2\left(\frac{\delta_t^u}{\delta_t}\right)^2\,\mathrm{d}t$, so skewing the range to the right also increases the variance of the LP's position. On the other hand, if $\mu \leq 0$, then the LP reduces her losses by decreasing the value δ^u or equivalently increasing the value of δ^ℓ, i.e., by skewing her range of liquidity to the left. Thus, the LP uses the expected changes in the marginal rate to skew the range of liquidity and to increase her terminal wealth.

3.2. Fee income

In this section, we first show that fee income is subject to a tradeoff between the spread δ of the LP's position and PL, which scales with the volatility of Z. Next, we show how the LP uses the expected changes in the marginal rate given by the stochastic drift μ to skew her liquidity around Z. Finally, we propose dynamics for the LP's fee income that we use in our model.

3.2.1. Fee income: spread, concentration risk, and pool fee rate

In the three cases of (1), increasing the spread of the LP's position reduces the depth $\tilde{\kappa}$ of the LP's position in the pool. Recall that the LP fee income is proportional to $\tilde{\kappa}/\kappa$, where κ is the pool depth. Thus, decreasing the value of $\tilde{\kappa}$ potentially reduces LP fee income because the LP holdings

Electronic copy available at: https://ssrn.com/abstract=4273989

represent a smaller portion of the pool depth around the rate Z. Figure 4 shows the value of $\tilde{\kappa}$ as a function of the spread δ.

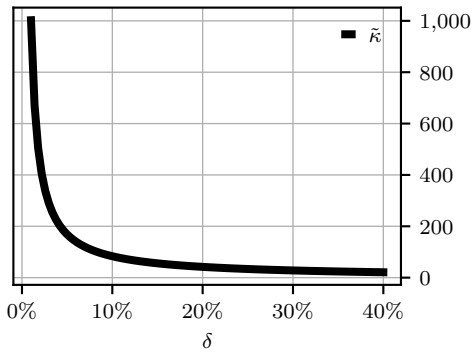

Figure 4: Value of the depth $\tilde{\kappa}$ of the LP's position in the pool as a function of the spread δ. The spread is in percentage of the marginal exchange rate; recall that $\left(Z_t^u - Z_t^\ell\right)/Z_t \approx \delta_t$.

However, although narrow ranges increase the potential fee income, they also increase concentration risk; a wide spread (i.e., a lower value of the depth $\tilde{\kappa}$) decreases fee income per LT transaction but reaps earnings from a larger number of LT transactions because the position is active for longer periods of time (i.e., it takes longer, on average, for Z to exit the LP's range). Thus, the LP must strike a balance between maximising the depth $\tilde{\kappa}$ around the rate and minimising the concentration risk, which depends on the volatility of the rate Z.

The dynamics of the fee income in our model of Section 4 uses a fixed depth κ and assumes that the pool generates fee income for all LPs at an instantaneous *pool fee rate* π; clearly, these fees are paid by LTs who interact with the pool. The value of π represents the instantaneous profitability of the pool, akin to the size of market orders and their arrival rate in LOBs.

To analyse the dynamics of the pool fee rate π, we use historical LT transactions in Uniswap v3 as a measure of activity and to estimate the total fee income generated by the pool; Appendix A describes the data and Table A.4 provides descriptive statistics. Figure 5 shows the estimated fee rate π in the ETH/USDC pool. For any time t, we use

$$\pi_t = 0.05\% \, \frac{V_t}{2\,\kappa\, Z_t^{1/2}} \,,$$

where V_t is the volume of LT transactions the day before t, $2\,\kappa\, Z_t^{1/2}$ is the pool value in terms of asset X at time t, and 0.05% is the fixed fee of the pool.[2] Figure 5 suggests that the pool fee

[2]The value of a CPM pool is given by the active pool depth. In particular, the size of a pool with quantity x of asset X and quantity y of asset Y is $x + Z\,y = 2\,x = 2\,\kappa\, Z^{1/2}$ units of X because $x\,y = \kappa^2$ and $Z = x/y \implies x^2 = \kappa^2\, Z$.

Electronic copy available at: https://ssrn.com/abstract=4273989

rate π generated by liquidity taking activity in the pool is stochastic and mean reverting. Here, we assume that π is independent of the rate Z over the time scales we consider; see Table 1.

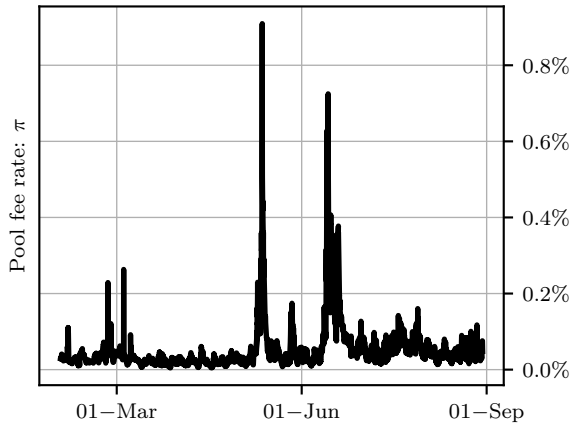

Figure 5: Estimated pool fee rate from February to August 2022 in the ETH/USDC pool. For any time t, the pool fee rate is the total fee income, as a percentage of the total pool size, paid by LTs on the period $[t - 1 \text{ day}, t]$. The pool size at time t is $2\,\kappa\,Z_t^{1/2}$ in terms of asset X, where Z_t is the active rate in the pool at time t.

	$\Delta t = 1$ minute	$\Delta t = 5$ minutes	$\Delta t = 1$ hour	$\Delta t = 1$ day
Correlation	-2.1%	-2.4%	-2.6%	-10.9%

Table 1: Correlation of the returns of the rate Z and the fee rate π, i.e., $(Z_{t+\Delta t} - Z_t)/Z_t$ and $(Z_{t+\Delta t} - Z_t)/Z_t$ for $\Delta t = 1$ minute, five minutes, one hour, and one day, using data of the ETH/USDC pool between 5 May 2021 and 18 August 2022.

In our model, the LP continuously adjusts her position around the current rate Z, so we write the continuous-time dynamics of (2), conditional on the rate not exiting the LP's range, as

$$\mathrm{d}p_t = \underbrace{(\tilde{\kappa}_t \,/\, \kappa)}_{\text{Position depth}} \underbrace{\pi_t}_{\text{Fee rate}} \underbrace{2\,\kappa\,Z_t^{1/2}}_{\text{Pool size}} \mathrm{d}t\,,$$

where $(\tilde{\kappa}_t)_{t\in[0,T]}$ models the depth of the LP's position and p is the LP's fee income for providing liquidity with depth $\tilde{\kappa}$ in the pool. The fee income is proportional to the pool size, i.e., proportional to $2\,\kappa\,Z_t^{1/2}$. Next, use the second equation in (1) and equations (6)–(4) to write the dynamics of the LP's position depth $\tilde{\kappa}_t$ as

$$\tilde{\kappa}_t = 2\,\tilde{x}_t \left(\frac{1}{\delta_t^{\ell} + \delta_t^{u}}\right) Z_t^{-1/2}\,,$$

Electronic copy available at: https://ssrn.com/abstract=4273989

so the dynamics in (8) become

$$\mathrm{d}p_t = \left(\frac{4}{\delta_t^\ell + \delta_t^u}\right) \pi_t \, \tilde{x}_t \, \mathrm{d}t \, . \tag{8}$$

In practice, the LP chooses how often to reposition her liquidity. Thus, the LP faces the risk that the rate exits the spread around Z in between the times the LP repositions her liquidity. Clearly, the continuous-time dynamics in (8) do not take into account concentration risk. In practice, narrow spreads generate less fee income because the rate Z may exit the range of the LP's liquidity, especially in volatile markets. Thus, we introduce a concentration cost to reduce the fees collected by the LP. The concentration costs increase (decrease) when the spread narrows (widens), so we modify the dynamics of the fees collected by the LP in (8) to account for the concentration cost and write

$$\mathrm{d}p_t = \left(\frac{4}{\delta_t^\ell + \delta_t^u}\right) \pi_t \, \tilde{x}_t \, \mathrm{d}t \; - \gamma \left(\frac{1}{\delta_t^\ell + \delta_t^u}\right)^2 \tilde{x}_t \, \mathrm{d}t \, , \tag{9}$$

where $\gamma > 0$ is the concentration cost parameter and $\tilde{x}_t$ is the wealth invested by the LP in the pool at time t.

Figure 6 compares the fee income from (8) and from (9), which includes the concentration cost, as a function of the spread of the LP's position. We simulate a driftless rate Z with $\sigma = 1\%$ and $\sigma = 3\%$ and assume that the LP adjusts her liquidity with a frequency of $\Delta t = 1$ minute. The fee income corresponding to every level of the spread is normalised by the maximum ex-post fee income (the normalised maximum fee revenue is 1). The figure shows that the concentration cost term in (9) captures the loss in fee revenue because of concentration risk. In addition, LPs should adapt the concentration cost parameter γ to the volatility of the rate Z. The LP can also choose the value of γ based on her beliefs about the future realised volatility.

In the remainder of this work, we assume that the pool fee rate process $(\pi)_{t\in[0,T]}$ follows the Cox–Ingersoll–Ross-type dynamics

$$\mathrm{d}(\pi_t - \eta_t) = \Gamma \, (\overline{\pi} + \eta_t - \pi_t) \, \mathrm{d}t + \psi \sqrt{\pi_t - \eta_t} \, \mathrm{d}B_t \, . \tag{10}$$

where $(\eta_t)_{t\in[0,T]}$ is a predictable process that we define below, $\Gamma > 0$ denotes the mean reversion speed, $\overline{\pi} > 0$ is the long-term mean of $(\pi_t - \eta_t)_{t\in[0,T]}$, $\psi > 0$ is a non-negative volatility parameter, $(B_t)_{t\in[0,T]}$ is a Brownian motion independent of $(W_t)_{t\in[0,T]}$, and $\pi_0 - \eta_0 > 0$ is known. In our

Electronic copy available at: https://ssrn.com/abstract=4273989

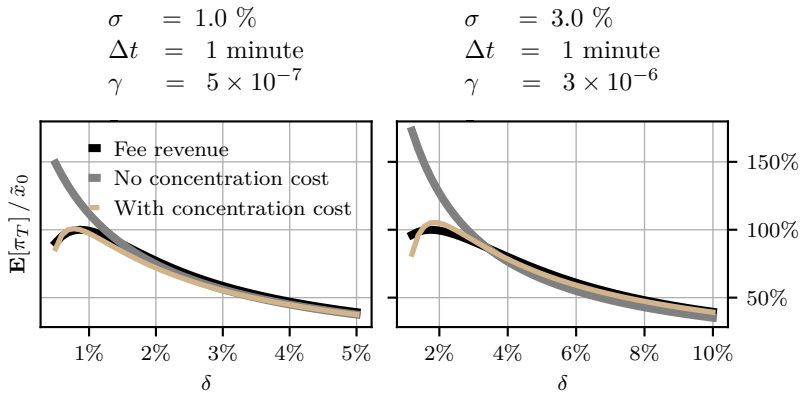

Figure 6: Fee income based on the dynamics in (8), without concentration cost (i.e., $\gamma = 0$), and in (9), with concentration cost $\gamma > 0$. We use simulations of the rate Z in (3) and assume π follows the mean-reverting process $\mathrm{d}\pi_t = a\,(b - \pi_t)\,\mathrm{d}t + c\,\mathrm{d}B_t$, where B_t is a standard Brownian motion independent of W. For the rate Z, we use $\mu = 0$, and $\sigma = 1\,\%$ and $3\,\%$. The parameters of the pool fee rate π, are obtained with maximum likelihood estimation from the fee rate of the ETH/USDC pool in Figure 5. We obtain $a = 2.71$, $b = 0.22\%$, and $c = 0.18$. For every spread value, we use (2) to obtain individual fee incomes and use (8) to obtain the expected terminal fee income.

model, we set

$$\eta_t = \frac{\sigma^2}{8} - \frac{\mu_t}{4}\left(\mu_t - \frac{\sigma^2}{2}\right) + \frac{\varepsilon}{4}\,. \tag{11}$$

From (10) it follows that

$$\pi_t - \eta_t \geq 0 \implies 4\,\pi_t - \frac{\sigma^2}{2} + \mu_t\left(\mu_t - \frac{\sigma^2}{2}\right) \geq \varepsilon > 0\,, \quad \forall t \in [0, T]\,, \tag{12}$$

which is a profitability condition that ensures that the spread δ of the optimal strategy derived below in Section 4 is well defined. Financially, the inequality in (12) guarantees that fee income is greater than the PL faced by the LP, adjusted by the drift in the marginal rate. The profitability condition (12) is further discussed in Section 4.3.

3.2.2. Fee income: drift and asymmetry

The stochastic drift μ indicates the future expected changes of the marginal exchange rate in the pool. In practice, the LP may use a predictive signal so μ represents the belief that the LP holds over the future marginal exchange rate in the pool. For an LP who maximises fee revenue, it is natural to consider asymmetric liquidity positions that capture the liquidity taking flow. We define the *asymmetry* of a position as

$$\rho_t = \delta_t^u \,/\, \left(\delta_t^u + \delta_t^\ell\right) = \delta_t^u / \delta_t\,, \tag{13}$$

Electronic copy available at: https://ssrn.com/abstract=4273989

where δ_t^u and δ_t^ℓ are defined in (4). In one extreme, when the asymmetry $\rho \to 0$, then $Z^u \to Z$ and the position consists of only asset X, and in the other extreme, when $\rho \to 1$, then $Z^\ell \to Z$ and the position consists of only asset Y.

In this section, we use Uniswap v3 data to study how the asymmetry and the width of the LP's range of liquidity relate to fee revenue. First, we estimate the realised drift μ in the pool ETH/USDC over a rolling window of $T = 5$ minutes.[3] Next, for any time t, the fee income for different positions of the LP's liquidity range is computed for various values of the spread δ and for various values of the asymmetry ρ. For each value of the realised drift μ during the investment horizon, and for each fixed value of the spread δ, we record the asymmetry that maximises fee income. Figure 7 shows the optimal (on average) asymmetry ρ as a function of the spread δ of the position for multiple values of the realised drift μ.

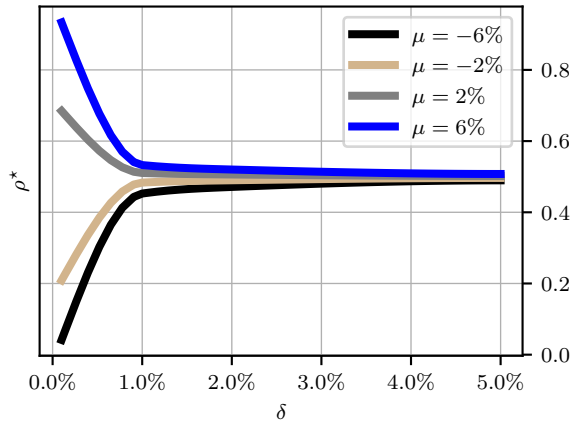

Figure 7: Optimal position asymmetry $\rho^\star$ in (13) as a function of the spread δ of the position, for multiple values of the drift μ. The asymmetry $\rho^\star$ is the value of ρ that maximises fee income for observed values of (δ, μ) .

Figure 7 suggests that there exists a preferred asymmetry of the position for a given value of the spread δ and a given value of the drift μ. First, for all values of the spread δ, the LP skews her position to the right when the drift is positive ($\rho^\star > 0.5$) and she skews her position to the left when the drift is negative ($\rho^\star < 0.5$). Second, for narrow spreads, the liquidity position requires more asymmetry than for large spreads when the drift is not zero. Clearly, an optimal liquidity provision model should take into account the drift μ and the spread of the position to adjust the asymmetry ρ.

In our liquidity provision model of Section 4, the LP holds a belief over the future exchange rate throughout the investment window and controls the spread $\delta = \delta^u + \delta^\ell$ of her position. Thus,

[3]The values of the drift in this section are normalised to reflect daily estimates. In particular, we use $\mu = \tilde{\mu} \,/\, \Delta t$ where $\tilde{\mu}$ is the average of the observed log returns and Δt is the observed average LT trading frequency.

Electronic copy available at: https://ssrn.com/abstract=4273989

she strategically chooses the asymmetry of her position as a function of δ and μ. We approximate the relationship exhibited in Figure 7 with the asymmetry function

$$\rho_t = \rho\left(\delta_t, \mu_t\right) = \frac{1}{2} + \frac{\mu_t}{\delta_t} = \frac{1}{2} + \frac{\mu_t}{\delta_t^u + \delta_t^\ell}, \quad \forall t \in [0, T]. \tag{14}$$

In the next section, we derive an optimal liquidity provision strategy, and prove that the profitability of liquidity provision is subject to a tradeoff between fee revenue, PL, and concentration risk.

4. Optimal liquidity provision in CL pools

4.1. The problem

Consider an LP who wants to provide liquidity in a CPM with CL throughout the investment window $[0, T]$. The LP implements a self-financing strategy that constantly repositions liquidity in a range $(Z_t^\ell, Z_t^u]$ around the active rate Z_t, which requires depositing and withdrawing liquidity continuously in the pool. The two ends of the spread, $(\delta_t^\ell)_{t\in[0,T]}$ and $(\delta_t^u)_{t\in[0,T]}$, are given in (4). The LP marks-to-market her holdings in terms of asset X. Throughout the trading window, the LP's wealth changes when the value of her holdings in the pool change. Her positions in the pool accumulate earnings from fees that she collects every time she withdraws her liquidity throughout the trading horizon.

We work on the filtered probability space $\left(\Omega, \mathcal{F}, \mathbb{P}; \mathbb{F} = (\mathcal{F}_t)_{t\in[0,T]}\right)$ where $\mathcal{F}_t$ is the natural filtration generated by the collection (Z, μ, π) and $[0, T]$ is the investment window. From the dynamics in (3) and (10), the LP also observes W and B, and η is determined by μ, so the LP observes all the stochastic processes of this problem.

The dynamics of the LP's wealth consist of the fees earned and the position value, i.e., the value of the LP's holdings in the pool. Similar to Section 3.1, we denote the wealth process of the LP by $(\tilde{x}_t = \alpha_t + p_t)_{t\in[0,T]}$, with $\tilde{x}_0 > 0$ known, and recall that $(\alpha_t)_{t\in[0,T]}$ is the value of the LP's position and $(p_t)_{t\in[0,T]}$ is the fee revenue. At any time t, the LP uses her wealth $\tilde{x}_t$ to provide liquidity, so the dynamics of the LP's position value are

$$\mathrm{d}\alpha_t = \tilde{x}_t \left(\frac{1}{\delta_t^\ell + \delta_t^u}\right)\left(-\frac{\sigma^2}{2}\,\mathrm{d}t + \mu_t\,\delta_t^u\,\mathrm{d}t + \sigma\,\delta_t^u\,\mathrm{d}W_t\right). \tag{15}$$

Throughout the investment window, we consider that the depth κ of the pool is constant and that liquidity taking activity in the pool generates fee income that is proportional to the pool size,

Electronic copy available at: https://ssrn.com/abstract=4273989

i.e., proportional to $2\,\kappa\,Z_t^{1/2}$. The proportion of the pool that is generated as fees, which we denote as the pool fee rate, is given by the process $(\pi_t)_{t\in[0,T]}$; see (9). Thus, the pool generates a quantity $2\,\kappa\,Z_t^{1/2}\,\pi_t\,\mathrm{d}t$ in terms of asset X over an infinitesimal time step, which is distributed among LPs proportionally to the liquidity $\tilde{\kappa}_t$ they hold in the pool. The fee income of the agent evolves as

$$\mathrm{d}p_t = \left(\frac{4}{\delta_t^\ell + \delta_t^u}\right)\,\pi_t\,\tilde{x}_t\,\mathrm{d}t - \gamma\,\left(\frac{1}{\delta^\ell + \delta^u}\right)^2\,\tilde{x}_t\,\mathrm{d}t\,,$$

and recall that $\gamma \geq 0$ is the concentration cost parameter; see Subsection 3.2. Thus, the dynamics of the LP's wealth $\tilde{x} = \alpha + p$ are given by

$$\mathrm{d}\tilde{x}_t = \tilde{x}_t\,\left(\frac{1}{\delta_t^\ell + \delta_t^u}\right)\,\left[-\frac{\sigma^2}{2}\,\mathrm{d}t + \mu_t\,\delta_t^u\,\mathrm{d}t + 4\,\pi_t\,\mathrm{d}t + \sigma\,\delta_t^u\,\mathrm{d}W_t\right] - \gamma\,\left(\frac{1}{\delta_t^\ell + \delta_t^u}\right)^2\,\tilde{x}\,\mathrm{d}t\,, \quad (16)$$

where π follows the dynamics in (10).

As discussed in Section 3.2, the LP uses the stochastic drift μ to improve trading performance so she adjusts the asymmetry $\delta_t^u\,/\,\delta_t$ as a function of μ_t and the spread δ_t of her position, and we write $\rho_t = \rho\,(\mu_t, \delta_t)$ where $\rho \in \mathcal{C}^1\,(\mathbb{R}\times\mathbb{R}, \mathbb{R})$ is a deterministic function; see Subsection 3.2. Next, use $\delta_t = \delta_t^u + \delta_t^\ell$ and $\delta_t^u\,/\,\delta_t = \rho\,(\mu_t, \delta_t)$ in (16) to write the dynamics of the LP's wealth as

$$\mathrm{d}\tilde{x}_t = \frac{1}{\delta_t}\,\left(4\,\pi_t - \frac{\sigma^2}{2}\right)\,\tilde{x}_t\,\mathrm{d}t + \mu_t\,\rho\,(\delta_t, \mu_t)\,\tilde{x}_t\,\mathrm{d}t + \sigma\,\rho\,(\delta_t, \mu_t)\,\tilde{x}_t\,\mathrm{d}W_t - \frac{\gamma}{\delta_t^2}\,\tilde{x}_t\,\mathrm{d}t\,.$$

4.2. The optimal strategy

The LP controls the spread δ of her position to maximise the expected utility of her terminal wealth in units of X, and the set of admissible strategies is

$$\mathcal{A}_t = \left\{(\delta_s)_{s\in[t,T]},\ \mathbb{R}\text{-valued},\ \mathbb{F}\text{-adapted, and}\ \int_t^T |\delta_s|^2\,\mathrm{d}s < +\infty\ \mathbb{P}\text{–a.s.}\right\}$$

with $\mathcal{A} := \mathcal{A}_0$.

Let $\delta \in \mathcal{A}$. The performance criterion of the LP is a function $u^\delta\colon [0,T]\times\mathbb{R}^4 \to \mathbb{R}$ given by

$$u^\delta(t, \tilde{x}, z, \pi, \mu) = \mathbb{E}_{t,\tilde{x},z,\pi,\mu}\left[U\left(\tilde{x}_T^\delta\right)\right]\,,$$

where U is a concave utility function, and the value function $u : [0,T]\times\mathbb{R}^4 \to \mathbb{R}$ of the LP is

$$u(t, \tilde{x}, z, \pi, \mu) = \sup_{\delta\in\mathcal{A}} u^\delta(t, \tilde{x}, z, \pi, \mu)\,. \quad (17)$$

Electronic copy available at: https://ssrn.com/abstract=4273989

The following results solve the optimal liquidity provision model when the LP assumes a general stochastic drift μ and adopts a logarithmic utility.

Proposition 1. *Assume the asymmetry function ρ is as in (14) and that $U(x) = \log(x)$. Then the function w given by*

$$
\begin{aligned}
w\left(t, \tilde{x}, z, \pi, \mu\right) = & \log\left(\tilde{x}\right) + \left(\pi - \eta\right)^2 \int_t^T \mathbb{E}_{t,\mu}\left[\frac{8}{2\,\gamma + \mu_s^2\,\sigma^2}\right] \exp\left(-2\,\Gamma\left(s-t\right)\right) \mathrm{d}s \\
& + \left(\pi - \eta\right)\left(2\,\Gamma\,\overline{\pi} + \psi^2\right) \int_t^T \mathbb{E}_{t,\mu}\left[C\left(s, \mu_s\right)\right] \exp\left(-\Gamma\left(s-t\right)\right) \mathrm{d}s \\
& - \left(\pi - \eta\right) \int_t^T \mathbb{E}_{t,\mu}\left[\frac{4\,\varepsilon}{2\,\gamma + \sigma^2\,\mu_s^2}\right] \exp\left(-\Gamma\left(s-t\right)\right) \mathrm{d}s \\
& + \int_t^T \left(\Gamma\,\overline{\pi}\,\mathbb{E}_{t,\mu}\left[E\left(s, \mu_s\right)\right] + \psi^2\,\mathbb{E}_{t,\mu}\left[\eta_s\,C\left(s, \mu_s\right)\right]\right) \mathrm{d}s \\
& - \int_t^T \left(\mathbb{E}_{t,\mu}\left[\frac{1}{2}\frac{\varepsilon^2}{2\,\gamma + \sigma^2\,\mu_s^2} + \frac{\mu_s}{2}\right]\right) \mathrm{d}s - \pi\frac{\sigma^2}{8}\left(T - t\right) ,
\end{aligned}
\tag{18}
$$

where $\eta_s = \frac{\sigma^2}{8} - \frac{\mu_s}{4}\left(\mu_s - \frac{\sigma^2}{2}\right) + \frac{\varepsilon}{4}$, $\eta = \frac{\sigma^2}{8} - \frac{\mu}{4}\left(\mu - \frac{\sigma^2}{2}\right) + \frac{\varepsilon}{4}$, $\mathbb{E}_{t,\mu}$ represents expectation conditioned on $\mu_t = \mu$ (or $\eta_t = \eta$), and

$$
C\left(t, \mu\right) = \mathbb{E}_{t,\mu}\left[\int_t^T \frac{8}{2\,\gamma + \mu_s^2\,\sigma^2} \exp\left(-2\,\Gamma\left(s-t\right)\right) \mathrm{d}s\right] ,
$$

and

$$
E\left(t, \mu\right) = \mathbb{E}_{t,\mu}\left[\int_t^T \left(\left(2\,\Gamma\,\overline{\pi} + \psi^2\right) C\left(s, \mu\right) + \frac{4\,\varepsilon}{2\,\gamma + \sigma^2\,\mu_s^2}\right) \exp\left(-\Gamma\left(s-t\right)\right) \mathrm{d}s\right] ,
$$

solves the HJB equation associated with problem (17).

For a proof, see Appendix B.1.

Theorem 1. *Assume the asymmetry function ρ is as in (14) and that $U(x) = \log(x)$. Then, the solution in Proposition 1 is the unique solution to the optimal control problem (17), and the optimal spread $(\delta_s)_{s\in[t,T]} \in \mathcal{A}_t$ is given by*

$$
\delta_s^\star = \frac{2\,\gamma + \mu_s^2\,\sigma^2}{4\,\pi_s - \frac{\sigma^2}{2} + \mu_s\left(\mu_s - \frac{\sigma^2}{2}\right)} = \frac{2\,\gamma + \mu_s^2\,\sigma^2}{4\left(\pi_s - \eta_s\right) + \varepsilon} ,
\tag{19}
$$

where $\eta_s = \frac{\sigma^2}{8} - \frac{\mu_s}{4}\left(\mu_s - \frac{\sigma^2}{2}\right) + \frac{\varepsilon}{4}$.

Electronic copy available at: https://ssrn.com/abstract=4273989

For a proof, see Appendix B.2.

4.3. Discussion: profitability, PL, and concentration risk

In this section, we study how the strategy depends on various model parameters (volatility σ of the pool's marginal rate, fees paid to the LP, and terminal date T) when $\mu \equiv 0$. When the LP does not assume a stochastic drift, the position is symmetric so $\rho = 1/2$ and $\delta_t^u = \delta_t^\ell = \delta_t/2$,[4] so the optimal spread (19) becomes

$$\delta_t^{\ell\star} = \delta_t^{u\star} = \frac{2\,\gamma}{8\,\pi_s - \sigma^2} \quad \Longrightarrow \quad \delta_t^\star = \frac{4\,\gamma}{8\,\pi_s - \sigma^2} \tag{20}$$

and the inequality in (12) becomes

$$4\,\pi_t - \frac{\sigma^2}{2} \geq \varepsilon > 0\,, \quad \forall t \in [0, T]\,. \tag{21}$$

The inequality in (21) guarantees that the optimal control (20) does not explode, and ensures that fee income is large enough for LP activity to be profitable. In particular, it ensures that $\pi > \sigma^2/8 + \varepsilon$. Note that when $\varepsilon \to 0$, i.e., when $\sigma^2/4 \to \pi$, the spread $\delta \to +\infty$. However, we require that the spread $\delta = \delta^u + \delta^\ell \leq 4$. Note that $\delta = 4$ when $\delta^\ell = \delta^u = 2$, so the conditions $\delta^\ell \leq 2$ and $\delta^u \leq 2$ become

$$\frac{\gamma}{4\,\pi - \frac{\sigma^2}{2}} \leq 2 \implies \pi - \frac{\gamma}{8} \geq \frac{\sigma^2}{8}\,. \tag{22}$$

When $\delta^\ell = \delta^u = 2$, the LP provides liquidity in the maximum range $(0\,, +\infty)$, so the depth of her liquidity position $\tilde{\kappa}$ is minimal, the PL is minimal, and the LP's position is equivalent to providing liquidity in CPMs without CL; see Cartea et al. (2023) for more details. In that case, the dynamics of PL in (7) are

$$\mathrm{dPL}_t = -\frac{\sigma^2}{8}\,\alpha_t\,\mathrm{d}t\,,$$

so $\sigma^2/8$ is the lowest rate at which the LP's assets can depreciate due to PL.

On the other hand, when $\delta \leq 4$, the depreciation rate of the LP's position value in (7) is higher. In particular, if $\delta = \delta^{\text{tick}}$, where δ^{tick} is the spread of a liquidity position concentrated within a single tick range, then the depth of the LP's liquidity position $\tilde{\kappa}$ is maximal and the PL is maximal.

[4] The position range is approximately symmetric around the position rate Z because $\delta_t^u = \delta_t^\ell$ does not imply that $Z - Z^\ell = Z^u - Z$; see (4). However, for small values of δ^ℓ and δ^u, one can write the approximation $Z - Z^\ell \approx Z^u - Z$, in which case the position is symmetric around the rate Z.

Electronic copy available at: https://ssrn.com/abstract=4273989

In that case, the dynamics of PL in (7) are

$$\mathrm{dPL}_t = -\frac{\sigma^2}{2\,\delta^{\text{tick}}}\,\alpha_t\,\mathrm{d}t\,,$$

so $\sigma^2/2\,\delta^{\text{tick}}$ is the highest rate at which the LP's assets can depreciate due to PL.

LPs should track the profitability of the pools they consider and check if the expected fee revenue covers PL before considering depositing their assets in the pool. When $\mu = 0$, we propose that LPs use $\sigma^2/8$ as a rule-of-thumb threshold for the pool's rate of profitability because $\sigma^2/8$ is the lowest rate of depreciation of their wealth in the pool.

The condition in (22) ensures that the profitability $\pi - \gamma/8$, which is the pool fee rate adjusted by the concentration cost, is higher than the depreciation rate of the LP's assets in the pool. Thus, the condition imposes a minimum profitability level of the pool, so LP activity is viable. An optimal control $\delta^\star > 4$ indicates non-viable LP activity because fees are not enough to compensate for the PL borne by the LP. Figure 8 shows the estimated pool fee rate and the estimated depreciation rate in the ETH/USDC pool (from January to August 2022). In particular, the CIR model captures the dynamics of $\pi_t - \sigma^2/8$.

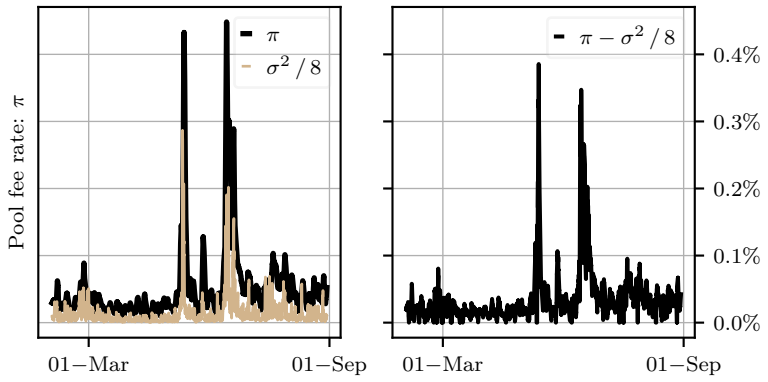

Figure 8: Estimated pool fee rate from February to August 2022 in the ETH/USDC pool. For any time t, the pool fee rate is the total fee income, as a percentage of the total pool size, paid by LTs in the period $[t - 1\text{ day}, t]$. The pool size at time t is $2\,\kappa\,Z_t^{1/2}$ where Z_t is the active rate in the pool at time t.

Next, we study the dependence of the optimal spread on the value of the concentration cost coefficient γ, the fee rate π, and the volatility σ. The concentration cost coefficient γ scales the spread linearly in (20). Recall that the cost term penalises small spreads because there is a risk that the rate will exit the LP's range. Thus, large values of γ generate large values of the spread. Figure 9 shows the optimal spread as a function of the pool fee rate π. Large potential fee income pushes the strategy towards targeting more closely the marginal rate Z to profit from fees. Finally,

Electronic copy available at: https://ssrn.com/abstract=4273989

Figure 10 shows that the optimal spread increases as the volatility of the rate Z increases.

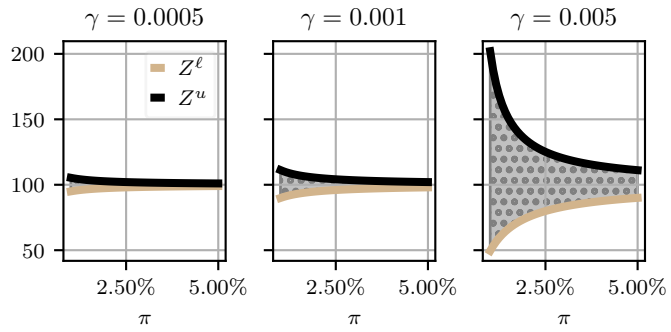

Figure 9: Optimal LP position range $\left(Z^\ell, Z^u\right]$ as a function of the pool fee rate π for different values of the concentration cost parameter γ, when $Z = 100$, $\sigma = 0.02$, and $\mu = 0$.

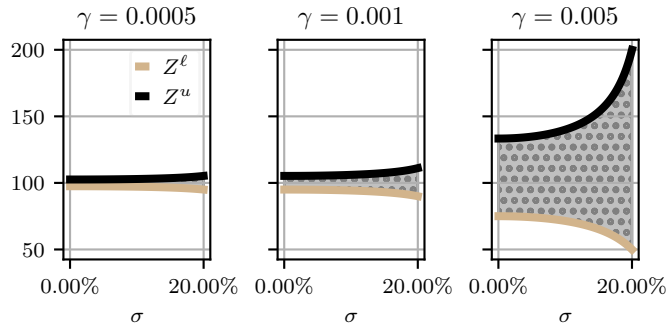

Figure 10: Optimal LP position range $\left(Z^\ell, Z^u\right]$ as a function of the volatility σ for different values of the concentration cost parameter γ, when $Z = 100$, $\pi = 0.02$, and $\mu = 0$.

Finally, the optimal spread does not depend on time or the terminal date T. Note that the LP marks-to-market her wealth in units of X, but does not penalise her holdings in asset Y. In particular, the LP's performance criterion does not include a running penalty or a final liquidation penalty (to turn assets into cash or into the reference asset). For example, if at the end of the trading window the holdings in asset Y must be exchanged for X, then the optimal strategy would skew, throughout the trading horizon, the liquidity range to convert holdings in Y into X through LT activity.[5]

[5]In LOBs, one usually assumes that final inventory is liquidated with adverse price impact and that there is a running inventory penalty, thus market making strategies in LOBs depend on the terminal date T.

Electronic copy available at: https://ssrn.com/abstract=4273989

4.4. Discussion: drift and position skew

In this section, we study how the strategy depends on the stochastic drift μ. Use $\delta_t = \delta_t^\ell + \delta_t^u$ and $\rho\left(\delta_t, \mu_t\right) = \delta_t^u / \delta_t$ to write the two ends of the optimal spread as

$$\delta_t^{u\star} = \frac{2\,\gamma + \mu_t^2\,\sigma^2}{8\,\pi_t - \sigma^2 + 2\,\mu_t\left(\mu_t - \frac{\sigma^2}{2}\right)} + \mu_t \quad \text{and} \quad \delta_t^{\ell\star} = \frac{2\,\gamma + \mu_t^2\,\sigma^2}{8\,\pi_t - \sigma^2 + 2\,\mu_t\left(\mu_t - \frac{\sigma^2}{2}\right)} - \mu_t\,. \tag{23}$$

The inequality in (12) guarantees that the optimal control in (23) does not explode and ensures that fee income is large enough for LP activity to be profitable. The profitability condition in (22) becomes

$$\pi_t - \frac{\gamma}{8} \geq \frac{\sigma^2}{8}\left(\frac{\mu_t^2}{2} + 1\right) - \frac{\mu_t}{4}\left(\mu_t - \frac{\sigma^2}{2}\right)\,,$$

so LPs that assume a stochastic drift in the dynamics of the exchange rate Z should use this simplified measure of the depreciation rate due to PL as a rule-of-thumb before considering depositing their assets in the pool.

Next, we study the dependence of the optimal spread on the value of the drift μ. First, recall that the controls in (23) must obey the inequalities[6]

$$0 < \delta_t^\ell \leq 2 \quad \text{and} \quad 0 \leq \delta_t^u < 2\,,$$

because $0 \leq Z^\ell < Z^u < \infty$ and $Z_t \in (Z_t^\ell, Z_t^u]$, which together with (5) implies $0 \leq \delta_t \leq 4$. Next, the asymmetry function satisfies

$$0 < \rho\left(\delta_t, \mu\right) = \frac{\delta_t^u}{\delta_t} < 1\,, \tag{24}$$

which implies

$$0 \leq \rho\left(\delta_t, \mu\right)\,\delta_t < 2 \quad \text{and} \quad 0 \leq \left(1 - \rho\left(\delta_t, \mu\right)\right)\,\delta_t < 2\,. \tag{25}$$

Now, use (14) and (25) to write

$$0 \leq \left(\frac{1}{2} + \frac{\mu}{\delta_t}\right)\,\delta_t < 2 \quad \text{and} \quad 0 \leq \left(\frac{1}{2} - \frac{\mu}{\delta_t}\right)\,\delta_t < 2\,. \tag{26}$$

Finally, use (24) and (26) to obtain the inequalities

$$2\,|\mu| \leq \delta_t \leq 4 - 2\,|\mu|\,, \tag{27}$$

[6]The admissible set of controls is not restricted to these ranges. However, values outside these range cannot be implemented in practice.

Electronic copy available at: https://ssrn.com/abstract=4273989

so μ must be in the range $[-1, 1]$ for the LP to provide liquidity. If μ is outside this range, concentration risk is too high so the LP must withdraw her holdings from the pool. Recall that the dynamics of Z are geometric and μ is a percentage drift, so values of μ outside the range $[-1, 1]$ are unlikely. Moreover, when $\mu = -1$, the drift of the exchange rate Z is large and negative so the optimal range is $(0, Z]$, i.e., the largest possible range to the left of Z. When $\mu = 1$, the drift of the exchange rate Z is large and positive so the optimal range is $(Z, +\infty)$, which is the largest possible range to the right of Z. Condition (27) is always verified when we study the performance of the strategy in the ETH/USDC pool. Figure 11 shows how the optimal spread adjusts to the value of the drift μ. Finally, note that

$$\frac{\partial \delta^{u\star}}{\partial \sigma} = \frac{\partial \delta^{\ell\star}}{\partial \sigma} = \frac{2\,\mu^2\,\sigma\,(4\,\pi - 4\,\eta + \varepsilon) + 4\,\sigma\,(1+\mu)\,(2\,\gamma + \mu^2\,\sigma^2)}{(4\,\pi - 4\,\eta + \varepsilon)^2} > 0\,, \qquad \forall \mu \in [-1, 1]\,,$$

shows that the optimal range is strictly increasing in the volatility σ of the rate Z, which one expects as increased activity that exposes the position value to more PL, and increases the concentration risk.

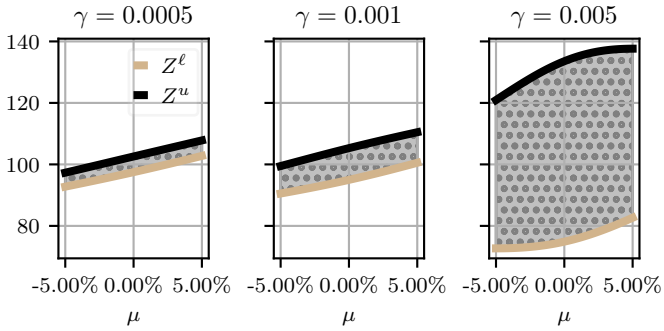

Figure 11: Optimal LP position range $\left(Z^\ell, Z^u\right]$ as a function of the drift μ for different values of the concentration cost parameter γ, when $Z = 100$, $\pi = 0.02$, and $\sigma = 0.02$.

5. Performance of strategy

5.1. Methodology

In this section, we use Uniswap v3 data between 1 January and 18 August 2022 (see data description in Appendix A) to study the performance of the strategy of Section 4. We consider execution costs and discuss how gas fees and liquidity taking activity in the pool affect the performance of

Electronic copy available at: https://ssrn.com/abstract=4273989

the strategy.[7]

Our strategy in Section 4 is solved in continuous time. In our performance study, we discretise the trading window in one-minute periods and the optimal spread is fixed at the beginning of each time-step. That is, let t_i be the times where the LP interacts with the pool, where $i \in \{1, \dots, N\}$ and $t_{i+1} - t_i = 1$ minute. For each time t_i, the LP uses the optimal strategy in (23) based on information available at time t_i, and she fixes the optimal spread of her position throughout the period $[t_i, t_{i+1})$; recall that the optimal spread is not a function of time.

To determine the optimal spread (23) of the LP's position at time t_i, we use in-sample data $[t_i - 1 \text{ day}, t_i]$ to estimate the parameters. The volatility σ of the rate Z is given by the standard deviation of one-minute log returns of the rate Z, which is multiplied by $\sqrt{1440}$ to obtain a daily estimate. The pool fee rate π_t is given by the total fee income generated by the pool during the in-sample period, divided by the pool size $2\,\kappa\,Z_t^{1/2}$ observed at time t, where κ is the observed active depth at time t. The concentration cost is $\gamma = 5 \times 10^{-7}$ and it penalises small spreads as shown in Figure 12. Finally, prediction of the future marginal rate Z is out of the scope of this work, thus we set $\mu = 0$ and $\rho = 0.5$.

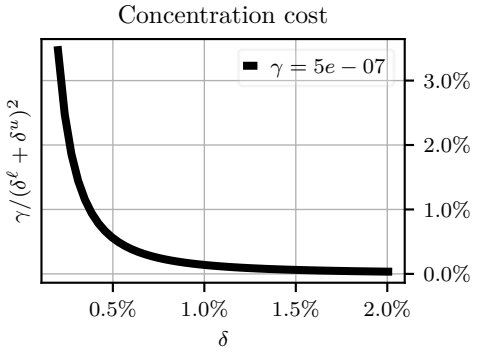

Figure 12: Concentration cost term γ/δ^2 as a function of the position spread when $\gamma = 5 \times 10^{-7}$, where $\delta = \delta^u + \delta^\ell$. The spread is in percentage of the marginal exchange rate; recall that $\left(Z_t^u - Z_t^\ell\right)/Z_t \approx \delta_t$.

To compute the LP's performance as a result of changes in the value of her holdings in the pool (position value), and as a result of fee income, we use out-of-sample data $[t_i, t_{i+1}]$. For the position value, we use equation (15) to determine the one-minute out-of-sample period. For fee income, we use LT transactions in the pool at rates included in the range $\left(Z_t^\ell, Z_t^u\right]$ and equation (2). The income from fees accumulates in a separate account in units of X with zero risk-free

[7] In practice, LPs pay gas fees when using the Ethereum network to deposit liquidity, withdraw liquidity, and adjust their holdings. Gas is paid in Ether, the native currency of the Ethereum network, and measures the computational effort of the LP operation; see Cartea et al. (2022).

Electronic copy available at: https://ssrn.com/abstract=4273989

rate.[8] At the end of the out-of-sample window, the LP withdraws her liquidity and earns the accumulated fees, and we repeat the in-sample estimation and out-of-sample liquidity provision described above. Thus, at times t_i, where $i \in \{1, \ldots, N-1\}$, the LP consecutively withdraws and deposits liquidity in different ranges. Between two consecutive operations (i.e., reposition liquidity provision), the LP may need to take liquidity in the pool to adjust her holdings in asset X and Y. In that case, we use results in Cartea et al. (2022) to compute execution costs.[9] In particular, we consider execution costs when the LP trades asset Y in the pool to adjust her holdings between two consecutive operations. More precisely, we consider that for every quantity y of asset Y bought or sold in the pool, a transaction cost $y\, Z_t^{3/2}/\kappa$ is incurred. We assume that the LP's taking activity does not impact the dynamics of the pool. Finally, we obtain 331,858 individual LP operations from 1 January to 18 August 2022.

5.2. Benchmark

We compare the performance of our strategy with the performance of LPs in the pool we consider. We select operation pairs that consist of first providing and then withdrawing the same depth of liquidity $\tilde{\kappa}$ at two different points in time by the same LP.[10] The operations that we select represent approximately 66% of all LP operations. Figure 13 shows the distribution of key variables that describe how LPs provide liquidity. The figure shows the distribution of the number of operations per LP, the changes in the position value, the length of time the position is held in the pool, and the position spread.

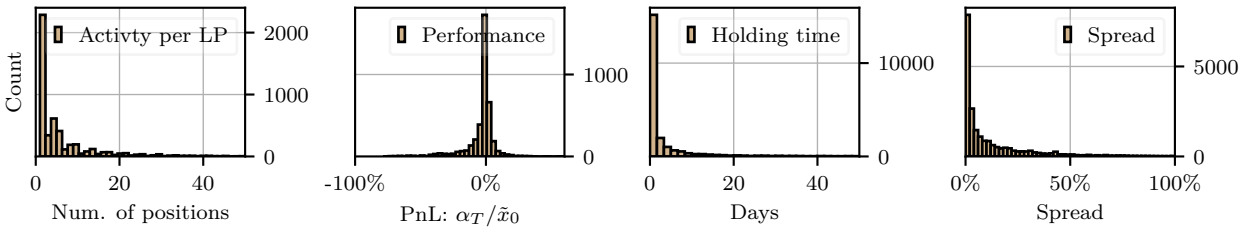

Figure 13: From left to right: distribution of the number of operations per LP, changes in the holdings value as a percentage of initial wealth, position hold time, and position spread. ETH/USDC pool with selected operations from 5,156 LPs between 5 May 2021 and 18 August 2022.

Finally, Table 2 shows the average and standard deviation of the distributions in Figure 13. Notice that the bulk of liquidity is deposited in small ranges, and positions are held for short

[8] In practice, fees accumulate in both assets X and Y.

[9] The authors in Cartea et al. (2022) show that execution costs in the pool are a closed-form function of the rate Z, the pool depth κ, and the transaction size.

[10] In blockchain data, every transaction is associated to a unique wallet address.

Electronic copy available at: https://ssrn.com/abstract=4273989

periods of time; 20% of LP positions are held for less than five minutes and 30% for less than one hour. Table 2 also shows that, on average, the performance of the LP operations in the pool and the period we consider is $-1.49\,\%$ per operation.

	Average	Standard deviation
Number of transactions per LP	11.5	40.2
Position value performance $(\alpha_T/\tilde{x}_0 - 1)$	-1.64%	7.5%
Fee income $(p_T/\tilde{x}_0 - 1)$	0.155%	0.274%
Hold time	6.1 days	22.4 days
Spread	18.7%	43.2%

Table 2: LP operations statistics in the ETH/USDC pool using operation data of 5,156 different LPs between 5 May 2021 and 18 August 2022. Performance includes transaction fees and excludes gas fees. The position value performance and the fee income are not normalised by the hold time.

5.3. Performance results

This subsection focuses on the performance of our strategy when gas fees are zero — at the end of the section we discuss the profitability of the strategy when gas fees are included. Figure 14 shows the distribution of the optimal spread (20) posted by the LP. The bulk of liquidity is deposited in ranges with a spread δ below 1%. Table 2 compares the average performance of the components of the optimal strategy with the performance of LP operations observed in the ETH/USDC pool.[11] Table 3 suggests that the position of the LP loses value in the pool (on average) because of PL; however, the fee income would cover the loss, on average, if one assumes that gas fees are zero. Finally, the results show that our optimal strategy significantly improves the PnL of LP activity in the pool and the performance of the assets themselves.

The results in Table 3 do not consider gas fees. Gas cost is a flat fee, so it does not depend on the position spread or size of transaction. If the activity of the LP does not affect the pool and if the fees collected scale with the wealth that the LP deposits in the pool, then the LP should consider an initial amount of X and Y that would yield fees enough to cover the flat gas fees. An estimate of the average gas cost gives an estimate of the minimum amount of initial wealth for a self-financing strategy to be profitable. Recall that, at any point in time t, the LP withdraws her

[11] In particular, performance is given for the selected operations shown in Figure 13.

Electronic copy available at: https://ssrn.com/abstract=4273989

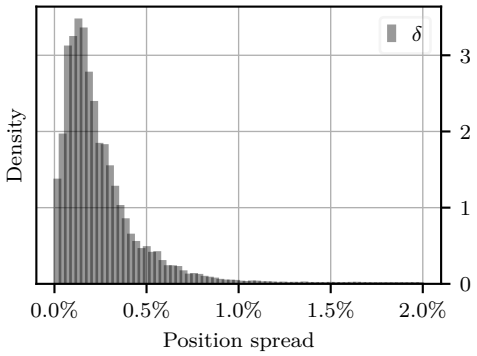

Figure 14: Distribution of the position spread δ.

liquidity, adjusts her holdings, and then deposits new liquidity. In the data we consider, the average gas fee is 30.7 USD to provide liquidity, 24.5 USD to withdraw liquidity, and 29.6 USD to take liquidity. Average gas costs are obtained from blockchain data which record the gas used for every transaction, and from historical gas prices. The LP pays a flat fee of 84.8 USD per operation when implementing the strategy in the pool we consider, so the LP strategy is profitable, on average, if the initial wealth deposited in the pool is greater than 1.8×10^6 USD.

Fee income of the LP strategy is limited by the volume of liquidity taking activity in the pool, so one should not only consider increasing the initial wealth to make the strategy more profitable. There are 4.7 LT transactions per minute and the average volume of LT transactions is $477,275$ USD per minute, so if the LP were to own 100% of the available liquidity, the average fee income per operation would be 1,431 USD.

Finally, our analysis did not take into account the impact of liquidity provision on liquidity taking activity, however, we expect liquidity provision in CPMs with CL to be profitable in pools where the volatility of the marginal rate is low, where liquidity taking activity is high, and when the gas fee cost to interact with the liquidity pools is low. These conditions ensure that the fees paid to LPs in the pool, adjusted by gas fees and concentration cost, exceed PL so liquidity provision is viable.

6. Conclusions

We studied the dynamics of the wealth of an LP in a CPM with CL who implements a self-financing strategy that dynamically adjusts the range of liquidity. The wealth of the LP consists of the position value and fee revenue. We showed that the position value depreciates due to PL and the LP widens her liquidity range to minimise her exposure to PL. On the other hand, the fee

Electronic copy available at: https://ssrn.com/abstract=4273989

	Position value performance per operation	Fee income per operation	Total performance per operation (with transaction costs, without gas fees)
Optimal strategy	-0.015% (0.0951%)	0.0197% (0.005%)	0.0047% (0.02%)
Market	-0.0024% (0.02%)	0.0017% (0.005%)	-0.00067% (0.02%)
Hold	n.a.	n.a.	-0.00016% (0.08%)

Table 3: **Optimal strategy**: Mean and standard deviation of the one-minute performance of the LP strategy (20) and its components. **Market**: Mean and standard deviation of one-minute performance of LP activity in the ETH/USDC pool using data between 1 January and 18 August 2022. **Hold**: Mean and standard deviation of the one-minute performance of holding the assets. In all cases, the performance includes transaction costs (pool fee and execution cost), but does not include gas fees.

revenue is higher for narrow ranges, but narrow ranges also increase concentration risk.

We derived the optimal strategy to provide liquidity in a CPM with CL when the LP maximises expected utility of terminal wealth. This strategy is found in closed-form for log-utility of wealth, and it shows that liquidity provision is subject to a profitability condition. In particular, the potential gains from fees, net of gas fees and concentration costs, must exceed PL. Our model shows that the LP strategically adjusts the spread of her position around the reference exchange rate; the spread depends on various market features including tthe volatility of the rate, the liquidity taking activity in the pool, and the drift of the rate.

Electronic copy available at: https://ssrn.com/abstract=4273989

Appendix A. Uniswap v3 ETH/USDC pool data statistics

ETH represents *Ether*, the Ethereum blockchain native currency. USDC represents *USD coin*, a currency fully backed by U.S. Dollars (USD). The fees paid by LTs is 0.05% of trade size; the fee is deducted from the quantity paid into the pool by the LT and distributed among LPs; see equation (2).

Uniswap v3 pools can be created with different values of the LT trading fee, e.g., 0.01%, 0.05%, 0.30%, or 1%, called fee tiers. Additionally, different pools with the same asset pair may coexist if they have different fee tiers. Once a pool is created, its fee tier does not change.

	LT	LP
Number of instructions	2,654,347	68,434
Average daily number of instructions	4,720	471
Total USD volume	$\approx$ \$ 262$\times 10^9$	$\approx$ \$ 232 $\times 10^9$
Average daily USD volume	\$ 554,624,500	\$ 863,285
Average LT transaction or LP operation size	\$ 98,624	\$ 3,611,197
Average interaction frequency	13 seconds	590 seconds

Table A.4: LT and LP activity in the ETH/USDC pool between 5 May 2021 and 18 August 2022: Total and average daily count of LT transactions and LP operations in the pool, total and average daily size of LT transactions and LP operations in the pool in USD, average LT transaction size and average LP operation size in USD dollars, and average liquidity taking and provision frequency.

Appendix B. Proofs

Appendix B.1. Proof of Proposition 1

To solve the problem (17), we introduce an equivalent control problem. First, define the process $(\tilde{\pi}_t)_{t\in[0,T]} = (\pi_t - \eta_t)_{t\in[0,T]}$ with dynamics

$$d\tilde{\pi}_t = \Gamma\ (\overline{\pi} - \tilde{\pi}_t)\,\mathrm{d}t + \psi\,\sqrt{\tilde{\pi}_t}\,\mathrm{d}B_t\,,$$

where $\tilde{\pi}_0 = \pi_0 - \eta_0$ and η is in (11).

We introduce the performance criterion $\tilde{u}^\delta\colon [0,T]\times\mathbb{R}^4 \to \mathbb{R}$ given by

$$\tilde{u}^\delta(t,\tilde{x},z,\pi,\mu) = \mathbb{E}_{t,\tilde{x},z,\tilde{\pi},\mu}\left[\log\left(\tilde{x}_T^\delta\right)\right]\,,$$

Electronic copy available at: https://ssrn.com/abstract=4273989

and the value function $\tilde{u} : [0,T] \times \mathbb{R}^4 \to \mathbb{R}$ given by

$$\tilde{u}(t,\tilde{x},z,\tilde{\pi},\mu) = \sup_{\delta\in\mathcal{A}} u^{\delta}(t,\tilde{x},z,\pi,\mu)\,. \tag{B.1}$$

Clearly, the problems (B.1) and (17) are equivalent, and the value functions satisfy $u(t,\tilde{x},z,\pi,\mu) = \tilde{u}(t,\tilde{x},z,\tilde{\pi},\mu)$ for all $(t,\tilde{x},z,\pi,\mu) \in: [0,T]\times\mathbb{R}^4$ and for all $\tilde{\pi} = \pi - \eta \in \mathbb{R}$, where $\eta = \frac{\sigma^2}{8} - \frac{\mu}{4}\left(\mu - \frac{\sigma^2}{2}\right) + \frac{\varepsilon}{4}$.

The value function in (B.1) admits the dynamic programming principle, so it satisfies the HJB equation

$$\begin{aligned} 0 = {} & \partial_t w + \frac{1}{2}\sigma^2 z^2\,\partial_{zz} w + \mu\, Z\,\partial_z w + \Gamma\left(\overline{\pi} - \tilde{\pi}\right)\partial_{\tilde{\pi}} w + \frac{1}{2}\,\psi^2\tilde{\pi}\partial_{\tilde{\pi}\tilde{\pi}} w + \mathcal{L}^{\mu} w \\ & + \sup_{\delta\in\mathbb{R}^+}\left(\frac{1}{\delta}\left(4\,\tilde{\pi} + 4\,\eta - \frac{\sigma^2}{2}\right)\tilde{x}\,\partial_{\tilde{x}} w + \mu\,\rho\left(\delta,\mu\right)\,\tilde{x}\,\partial_{\tilde{x}} w + \frac{1}{2}\,\sigma^2\,\rho\left(\delta,\mu\right)^2\,\tilde{x}^2\,\partial_{\tilde{x}\tilde{x}} w \right. \\ & \left. - \frac{\gamma}{\delta^2}\,\tilde{x}\,\partial_{\tilde{x}} w + \sigma^2\,\rho\left(\delta,\mu\right)\,\tilde{x}\,z\,\partial_{\tilde{x}z} w\right), \end{aligned} \tag{B.2}$$

with terminal condition

$$w(T,\tilde{x},z,\tilde{\pi},\mu) = \log\left(\tilde{x}\right), \quad \forall\left(\tilde{x},z,\tilde{\pi},\mu\right) \in \mathbb{R}^4,$$

where $\mathcal{L}^{\mu}$ is the infinitesimal generator of μ.

To study the HJB in (B.2), use the ansatz

$$w\left(t,\tilde{x},z,\tilde{\pi},\mu\right) = \log\left(\tilde{x}\right) + \theta\left(t,z,\tilde{\pi},\mu\right),$$

to obtain the HJB

$$\begin{aligned} 0 = {} & \partial_t\theta + \frac{1}{2}\sigma^2 z^2\,\partial_{zz}\theta + \mu\, Z\,\partial_z\theta + \Gamma\left(\overline{\pi} - \tilde{\pi}\right)\partial_{\tilde{\pi}} w + \frac{1}{2}\,\psi^2\tilde{\pi}\partial_{\tilde{\pi}\tilde{\pi}} w + \frac{\mu}{2} - \frac{1}{8}\,\sigma^2 \\ & + \mathcal{L}^{\mu}\theta + \sup_{\delta\in\mathbb{R}^+}\left(\frac{1}{\delta}\left(4\,\tilde{\pi} + 4\,\eta - \frac{\sigma^2}{2}\right) + \frac{\mu^2}{\delta} - \frac{1}{2}\,\sigma^2\left(\frac{\mu^2}{\delta^2} + \frac{\mu}{\delta}\right) - \frac{\gamma}{\delta^2}\right), \end{aligned} \tag{B.3}$$

with terminal condition

$$\theta\left(T,z,\tilde{\pi},\mu\right) = 0\,, \quad \forall(z,\tilde{\pi},\mu) \in \mathbb{R}^3\,.$$

Electronic copy available at: https://ssrn.com/abstract=4273989

The supremum in the HJB (B.3) is attained at

$$\delta^\star = \frac{2\,\gamma + \mu^2\,\sigma^2}{4\,\tilde{\pi} + 4\,\eta - \frac{\sigma^2}{2} + \mu\left(\mu - \frac{\sigma^2}{2}\right)} = \frac{2\,\gamma + \mu^2\,\sigma^2}{4\,\tilde{\pi} + \epsilon}\,.$$

Thus, (B.3) becomes

$$0 = \partial_t\theta + \frac{1}{2}\sigma^2\,z^2\,\partial_{zz}\theta + \mu\,Z\,\partial_z\theta + \Gamma\,(\overline{\pi} - \tilde{\pi})\,\partial_{\tilde{\pi}}\theta + \frac{1}{2}\,\psi^2\tilde{\pi}\partial_{\tilde{\pi}\tilde{\pi}}\theta + \frac{\mu}{2} - \frac{\sigma^2}{8} + \mathcal{L}^\mu\theta + \frac{1}{2}\frac{(4\,\tilde{\pi} + \epsilon)^2}{2\,\gamma + \mu^2\,\sigma^2}\,.$$

Next, substitute the ansatz

$$\begin{aligned}\theta\,(t, z, \tilde{\pi}, \mu) = {} & A\,(t,\mu)\,z^2 + B\,(t,\mu)\,\tilde{\pi}\,z + C\,(t,\mu)\,\tilde{\pi}^2 \\ & + D\,(t,\mu)\,z + E\,(t,\mu)\,\tilde{\pi} + F\,(t,\mu)\ ,\end{aligned}$$

in (B.3), collect the terms in Z and $\tilde{\pi}$, and write the following system of PDEs:

$$\begin{cases}(\partial_t + \mathcal{L}^\mu)\,A\,(t,\mu) = & -\sigma^2\,A\,(t,\mu) - 2\,\mu\,A\,(t,\mu)\ , \\ (\partial_t + \mathcal{L}^\mu)\,B\,(t,\mu) = & -\mu\,B\,(t,\mu) + \Gamma B\,(t,\mu)\ , \\ (\partial_t + \mathcal{L}^\mu)\,C\,(t,\mu) = & 2\,C\,(t,\mu)\,\Gamma - \frac{8}{2\,\gamma + \mu^2\,\sigma^2}\ , \\ (\partial_t + \mathcal{L}^\mu)\,D\,(t,\mu) = & -\mu\,D\,(t,\mu) - \Gamma\,\overline{\pi}\,B\,(t,\mu)\ , \\ (\partial_t + \mathcal{L}^\mu)\,E\,(t,\mu) = & -2\,\Gamma\,\overline{\pi}\,C\,(t,\mu) - \psi^2\,C\,(t,\mu) + \Gamma\,E\,(t,\mu) - \frac{4\,\varepsilon}{2\,\gamma + \sigma^2\,\mu^2}\ , \\ (\partial_t + \mathcal{L}^\mu)\,F\,(t,\mu) = & -\Gamma\,\overline{\pi}\,E\,(t,\mu) + \psi^2\,\eta\,C\,(t,\mu) - \frac{1}{2}\frac{\varepsilon^2}{2\,\gamma + \sigma^2\,\mu^2} - \frac{\mu}{2} + \frac{\sigma^2}{8}\ ,\end{cases}$$

with terminal conditions $A(T,\mu) = B(T,\mu) = C(T,\mu) = D(T,\mu) = E(T,\mu) = F(T,\mu) = 0$ for all $\mu \in \mathbb{R}$.

First, note that the PDEs in A, B, and D admit the unique solutions $A = B = D = 0$. Next, we solve the PDE in C. Use Itô's lemma to write

$$C\,(T, \mu_T) = C\,(t, \mu_t) + \int_t^T (\partial_t + \mathcal{L}^\mu)\,C\,(s, \mu_s)\,\mathrm{d}s\,.$$

Next, replace $(\partial_t + \mathcal{L}^\mu)\,C\,(s,\mu_s)$ with $2\,C\,(s,\mu_s)\,\Gamma - \frac{8}{2\,\gamma + \mu_s^2\,\sigma^2}$ to obtain

$$C\,(T, \mu_T) = C\,(t, \mu_t) + 2\,\Gamma\int_t^T C\,(s, \mu_s)\,\mathrm{d}s - \int_t^T \frac{8}{2\,\gamma + \mu_s^2\,\sigma^2}\,\mathrm{d}s\,.$$

Electronic copy available at: https://ssrn.com/abstract=4273989

Take expectations to get the equation

$$C\left(t,\mu_t\right)=\mathbb{E}_{t,\mu}\left[-2\,\Gamma\int_t^T C\left(s,\mu_s\right)\mathrm{d}s+\int_t^T\frac{8}{2\,\gamma+\mu_s^2\,\sigma^2}\,\mathrm{d}s\right].$$

Now consider the candidate solution function

$$\hat{C}\left(t,\mu_t\right)=\mathbb{E}_{t,\mu}\left[\int_t^T\frac{8}{2\,\gamma+\mu_s^2\,\sigma^2}\exp\left(-2\,\Gamma\left(s-t\right)\right)\,\mathrm{d}s\right]$$

and write

$$\begin{aligned}
&\mathbb{E}_{t,\mu}\left[-2\,\Gamma\int_t^T\hat{C}\left(s,\mu_s\right)\mathrm{d}s+\int_t^T\frac{8}{2\,\gamma+\mu_s^2\,\sigma^2}\,\mathrm{d}s\right]\\
=&\mathbb{E}_{t,\mu}\left[-2\,\Gamma\int_t^T\mathbb{E}_{t,\mu}\left[\int_s^T\frac{8}{2\,\gamma+\mu_u^2\,\sigma^2}\exp\left(-2\,\Gamma\left(u-s\right)\right)\,\mathrm{d}u\right]\mathrm{d}s+\int_t^T\frac{8}{2\,\gamma+\mu_s^2\,\sigma^2}\,\mathrm{d}s\right]\\
=&\mathbb{E}_{t,\mu}\left[\int_t^T\frac{8}{2\,\gamma+\mu_s^2\,\sigma^2}\exp\left(-2\,\Gamma\left(s-t\right)\right)\,\mathrm{d}s\right].
\end{aligned}$$

Thus $\hat{C}$ is a solution to the equation in C and by uniqueness of solutions, we conclude that $C=\hat{C}$.

Follow the same steps as above to obtain the solution

$$E\left(t,\mu\right)=\mathbb{E}_{t,\mu}\left[\int_t^T\left(\left(2\,\Gamma\,\overline{\pi}+\psi^2\right)C\left(s,\mu\right)+\frac{4\,\varepsilon}{2\,\gamma+\sigma^2\,\mu_s^2}\right)\exp\left(-\Gamma\left(s-t\right)\right)\,\mathrm{d}s\right]$$

to the PDE in E, and the solution

$$F\left(t,\mu\right)=\mathbb{E}_{t,\mu}\left[\int_t^T\left(\Gamma\,\overline{\pi}\,E\left(s,\mu_s\right)+\psi^2\,\eta_s\,C\left(s,\mu_s\right)-\frac{1}{2}\frac{\varepsilon^2}{2\,\gamma+\sigma^2\,\mu_s^2}-\frac{\mu_s}{2}+\frac{\sigma^2}{8}\right)\mathrm{d}s\right]$$

to the PDE in F, where $\eta_s=\frac{\sigma^2}{8}-\frac{\mu_s}{4}\left(\mu_s-\frac{\sigma^2}{2}\right)+\frac{\varepsilon}{4}$, which proves the result. □

Appendix B.2. Proof of Theorem 1

Proposition 1 provides a classical solution to (B.2). Therefore, standard results apply and showing that (19) is an admissible control is enough to prove that (18) is the value function (17). Specifically, use the form of the optimal control $\delta^\star$ in (19) and the dynamics for π in (10) to obtain

$$0<\delta_s^\star\leq\frac{\sigma^2\mu_s^2+2\,\gamma}{\varepsilon},\qquad\forall s\in\left[t,T\right],$$

Electronic copy available at: https://ssrn.com/abstract=4273989

thus $\delta^\star$ is an admissible control. □

References

Adams, H., Zinsmeister, N., Salem, M., Keefer, R., Robinson, D., 2021. Uniswap v3 core. Technical Report.

Angeris, G., Kao, H.T., Chiang, R., Noyes, C., Chitra, T., 2021. An analysis of uniswap markets.

Avellaneda, M., Stoikov, S., 2008. High frequency trading in a limit order book. Quantitative Finance 8, 217–224. doi:10.1080/14697680701381228.

Barger, W., Lorig, M., 2019. Optimal liquidation under stochastic price impact. International Journal of Theoretical and Applied Finance 22, 1850059.

Bergault, P., Drissi, F., Guéant, O., 2022. Multi-asset optimal execution and statistical arbitrage strategies under Ornstein–Uhlenbeck dynamics. SIAM Journal on Financial Mathematics 13, 353–390. doi:10.1137/21M1407756.

Bergault, P., Evangelista, D., Guéant, O., Vieira, D., 2021. Closed-form approximations in multi-asset market making. Applied Mathematical Finance 28, 101–142. doi:10.1080/1350486X.2021.1949359.

Cartea, Á., Donnelly, R., Jaimungal, S., 2017. Algorithmic trading with model uncertainty. SIAM Journal on Financial Mathematics 8, 635–671.

Cartea, Á., Donnelly, R., Jaimungal, S., 2018. Enhancing trading strategies with order book signals. Applied Mathematical Finance 25, 1–35.

Cartea, Á., Drissi, F., Monga, M., 2022. Decentralised finance and automated market making: Execution and speculation. Available at SSRN 4144743 .

Cartea, Á., Drissi, F., Monga, M., 2023. Predictable losses of liquidity provision in constant function markets and concentrated liquidity markets. Available at SSRN 4541034 .

Cartea, Á., Jaimungal, S., Penalva, J., 2015. Algorithmic and high-frequency trading. Cambridge University Press.

Cartea, Á., Jaimungal, S., Ricci, J., 2014. Buy low, sell high: A high frequency trading perspective. SIAM Journal on Financial Mathematics 5, 415–444.

Cartea, Á., Wang, Y., 2020. Market making with alpha signals. International Journal of Theoretical and Applied Finance 23, 2050016.

Chiu, J., Koeppl, T.V., 2019. Blockchain-based settlement for asset trading. The Review of Financial Studies 32, 1716–1753.

Donnelly, R., Lorig, M., 2020. Optimal trading with differing trade signals. Applied Mathematical Finance 27, 317–344.

Drissi, F., 2022. Solvability of differential Riccati equations and applications to algorithmic trading with signals. Available at SSRN 4308008 .

Drissi, F., 2023. Models of market liquidity: Applications to traditional markets and automated market makers. Available at SSRN 4424010 .

Fan, Z., Marmolejo-Cossio, F., Moroz, D.J., Neuder, M., Rao, R., Parkes, D.C., 2023. Strategic liquidity provision in uniswap v3. arXiv preprint arXiv:2106.12033 .

Forde, M., Sánchez-Betancourt, L., Smith, B., 2022. Optimal trade execution for Gaussian signals with power-law resilience. Quantitative Finance 22, 585–596.

Electronic copy available at: https://ssrn.com/abstract=4273989

Fukasawa, M., Maire, B., Wunsch, M., 2023. Model-free hedging of impermanent loss in geometric mean market makers. arXiv preprint arXiv:2303.11118 .

Guéant, O., 2016. The Financial Mathematics of Market Liquidity: From optimal execution to market making. volume 33. CRC Press.

Guéant, O., 2017. Optimal market making. Applied Mathematical Finance 24, 112–154. doi:10.1080/1350486X.2017.1342552.

Heimbach, L., Schertenleib, E., Wattenhofer, R., 2022. Risks and returns of Uniswap v3 liquidity providers.

Ho, T.S., Stoll, H.R., 1983. The dynamics of dealer markets under competition. The Journal of Finance 38, 1053–1074.

Lipton, A., Treccani, A., 2021. Blockchain and Distributed Ledgers: Mathematics, Technology, and Economics. World Scientific.

Milionis, J., Moallemi, C.C., Roughgarden, T., 2023. Automated market making and arbitrage profits in the presence of fees. arXiv preprint arXiv:2305.14604 .

Electronic copy available at: https://ssrn.com/abstract=4273989